Research article

Transcriptome profiling of barley and tomato shoot and root meristems unravels physiological variations underlying photoperiodic sensitivity

Authors: Michael Schneider[1,3] , Lucia Vedder[2] , Benedict Chijioke Oyiga [1] , Boby Mathew[1] , Heiko Schoof[2], Jens Léon[1], Ali Ahmad Naz[1,4*]

Affiliations:

[1]University of Bonn; Institute of Crop Science and Resource Conservation, Plant Breeding, Katzenburgweg 5, 53115 Bonn, Germany

[2]University of Bonn; Institute of Crop Science and Resource Conservation, Crop Bioinformatics, Katzenburgweg 2, 53115 Bonn, Germany

[3]Present address - Institute for Quantitative Genetics and Genomics of Plants, Heinrich Heine University, Universitätstrasse 1, 40225 Düsseldorf, Germany

[4]Present address – Institute of Agricultural Sciences and Landscape Architecture, University of Onsabrück, Germany

***Correspondence:** Ali Ahmad Naz; a.naz@hs-osnabrueck.de

Abbreviations

MACE - massive analysis of cDNA Ends sequencing

GO – gene ontology

LFC – log fold change

DEG – differentially expressed gene

EEG – equally expressed gene

Abstract

The average sowing date of crops in temperate climate zones has been shifted forwards by several days, resulting in a changed photoperiod regime at the emergence stage. In the present study, we performed a global transcriptome profiling of plant development genes in the seedling stage of root and shoot apical meristems of a photoperiod-sensitive species (barley) and a photoperiod insensitive species (tomato) in short-day conditions (8h). Variant expression indicated differences in physiological development under this short day-length regime between species and tissues. The barley tissue transcriptome revealed reduced differentiation compared to tomato. In addition, decreased photosynthetic activity was observed in barley, indicating a slower physiological development of shoot meristems than in tomatoes. The photomorphogenesis controlling cryptochrome gene *cry1*, with an effect on physiological differentiation, showed an underexpression in barley compared to tomato shoot meristems. This might lead to a cascade of suspended sink-source activities, which ultimately delay organ development and differentiation in barley shoot meristems under short photoperiods.

Keywords: Crops, Transcriptomics, Photoperiod, Interspecies comparison, Barley, Tomato

1. Introduction

Flowering plants are divided into two major classes - monocotyledons and dicotyledons. Significant diversification of these plants endured about 200 million years ago (1). In spite of a protracted evolutionary divergence, most cultivated crops are a member of these major categories. Barley and tomato are genomic models for crops that represent monocots and dicots, respectively. In addition, these species reveal characteristic differences in their development and growth habits, especially in the root and shoot forms. Thus, genomic dissection of this variation provides an opportunity to address critical biological questions behind the evolutionary and developmental divergence.

Roots are programmed in the root apical meristem and part of the elongation zone where the lateral root arises (2). Shoots develop in the shoot apical meristem and its peripheral location, where leaf primordial arises successively. A major factor determining the development rate is the phyllochron, which ultimately regulates branching (3). Besides the temperature as a significant factor determining the phyllochron (4), the photomorphogenesis is light-mediated (5). In Barley and Tomato, three ortholog cryptochrome-mediated light response genes were characterized and described (*Cry1a, Cry1b, Cry2*)(5). All of these have the function of photoreceptors in common (6), where *Cry1a* was described to significantly influence the partitioning of photoassimilates between roots and shoots in tomato (7). This underlines that although root and shoot develop and grow at different spots, active communication and exchange between both organs determines specific plant architecture (8,9).

Many photoperiod-regulated genes in barley have been described to affect development. The effect of photoperiod-sensitive alleles on the phyllochron and the prior-anthesis developmental phases in barley has been described before (10). This also highlights the high relevance of fast canopy and root establishment in Mediterranean climates. Little impact of photoperiod sensitive allele Ppd-H1 compared to reduced sensitive allele ppd-H1 regarding the pre-awn primordium stage developmental time variation was found (11).

Contrasting to barley, cultivated tomato is characterized by a day-length neutral growth habit (12). So far, the effect of photoperiod on the generative development and yield formation in crops has been illustrated (13,14). Still, little research was performed concerning vegetative development in early growth stages. The growing season extended by up to 20 days in the past decades (15,16), but little gains in biomass production were reported for photoperiod-sensitive species (17,18). The missing adaptation towards these changed growth conditions might cause yield reductions or counteract yield increases in new spring-type varieties. Especially with more frequent drought events observed, unproductive growth habits determined by the photoperiod are undesired (10). By comparing a photoperiod-dependent and independent species, developmental variations in root and shoot tissues should expose the effect of photoperiodic regulation in a short day length regime of 8h.

2. Materials and Methods

Plant material and experimental design for transcriptome analysis

Spring barley cultivar Scarlett and tomato cultivar Moneymaker were used as genotypes in the presented study. Seeds were pre-germinated and sown in soil in 96-cell plant growing trays. Plants were grown inside a growth chamber at 22°C for 8 hours light and 18°C for 16 hours night regime for ten days. Root and shoot apices were harvested the following day, pooling 50 individuals of the same genotype in each of the three biological replicates. Apices were dissected and separated under a microscope. The soil was removed carefully for the root apices by washing these in a petri dish in freshwater. Seven millimeters of primary roots containing the apical meristem and elongation zone of barley and tomato were harvested. The absence of root hairs determined the root elongation zone. Likewise, three biological replicates were harvested independently in each species. Barley vegetative shoot apices comprising apical meristem and emerging leaf primordia were dissected, and 50 shoot apices were pooled in each of the three biological replicates. Similarly, 50 tomato vegetative shoot apices, comprising shoot apical meristem and emerging leaf primordial, were collected. Samples were

harvested at similar time points on the same day in the laboratory and immediately frozen in liquid nitrogen after dissection.

RNA extraction and Massive Analysis of cDNA Ends (MACE) analysis

MACE-based transcriptome analysis was performed by GeneXpro GmbH (Frankfurt, Germany) (19). According to the manufacturer's description, the root and shoot tissues were homogenized, and total RNA was extracted for each sample using the INVITEK plant RNA mini kit (INIVTEK, Germany). RNA was fragmented, and polyadenylated mRNA was enriched by poly-A-specific reverse transcription. A specific adapter was ligated to the 5' ends, and the 3' ends were amplified by competitive PCR. MACE sequencing is based on the TrueQuant method, which reduces the amount of duplicate transcript sequencing and enables the precise comparison and identification of ultra-low expressed transcripts. Sequencing was performed on the Illumina platform (San Diego, USA).

Gene expression and function analyses

Transcriptome data were qualitatively adjusted using Trimmomatic SE (version 0.36)(20) with a minimum length of 40 bases and quality filter parameters of 28 for the leading and 17 for the trailing bases linked with a *head crop* of 10 bases. Fragments were aligned with the barley (IBSC_V2) and tomato (SL2.50) reference genome (21) using BWA mem (version 0.7.17)(22) applying standard settings. Read filtering was performed strictly, applying a quality filter of >60 using samtools 1.8 (23) view option. Duplicates as residuals from the PCR step in sequencing were disregarded due to the low impact in expression analysis (24)and the applied TrueQuant technique. Fragments were matched to the genes by the tool featurecounts of the subread software package (version 1.6.2) for tomato and barley separately, using the corresponding annotation files for the used reference (25).

Further analyses were performed in the R (3.4.4) (26)and Julia (1.5.1) (27) environments. The expressional and functional analysis methodology is presented in the workflow chart in figure S1. The read count normalization and probability values were calculated using Bioconductor package *edgeR* for transcriptome analysis (28,29). The analysis of both species was performed separately between the

root and shoot apical meristem transcriptomes. Probability (*p*) value adjustment was performed by R function *p.adjust*, once by false discovery rate (FDR) and Bonferroni adjustment. Analysis was further performed based on FDR. Replicate testing was done applying a generalized linear mixed model based on a negative binomial distribution. Differentially expressed genes (DEG) were selected based on FDR values of $p < 0.01$ and a log fold change (LFC) bigger 3. These were used to run a gene ontology (GO) enrichment by AgriGoV2 (30) with default settings. Additionally, the GO terms were compared based on the expression level of the genes. DEG were associated with corresponding GO terms,

$$expr_k = \frac{\sum CPM_{i_k}}{count(i_k)}$$

where the expression *CPM* of all genes *i,* annotated to the same GO term *k* were summarized to an average gene ontology expression $expr_k$. The expression pattern of the root and shoot group was compared in a generalized linear model (based on a negative binomial distribution),

$$p = glm\begin{bmatrix} a_{CPM_{1_k}} & b_{CPM_{1_k}} \\ \vdots & \vdots \\ a_{CPM_{n_k}} & b_{CPM_{n_k}} \end{bmatrix}, \text{expression ~ species}$$

where *p* is the probability derived from the *glm* model, which tests the gene expression *1:n* for GO term *k* in tissue *a* against tissue *b*. This step identified p values for GO terms based on the expression level. After FDR adjustment, candidate GO terms were selected by applying a cut-off of FDR < 0.01, LFC > 3, and a minimum of five genes per GO.

Subsequently, tomato and barley were directly compared on GO expression level, analog to the previously presented equation. Therefore, the gene expression values of the GO terms were matched for both barley and tomato tissues. The LFC between root and shoot of the same species was calculated and compared to the other species for each GO term. Therefore, the LFC distribution of each GO term was compared between tomato and barley. Differentially expressed GO terms were selected from this set based on an FDR < 0.05 and a gene count > 2.

Furthermore, orthologous genes were identified based on reference proteome sequence level using default settings of OrthoMCL (31). The minimum cut-off was set to an e-value threshold of $1e^{-5}$ and a length match of at least 50% for the essential all-vs-all BLASTP (32) step. The identified set of genes was used to match genes on a 1:1 base by the read count step onward. The genes were extracted from the raw read counting file. Root and shoot were separated so that barley and tomato were compared on both tissue levels separately by edgeR. The output of this was clustered in significantly DEG (FDR < 0.05, LFC > 3, normalized expression in both species >5) and equally expressed genes (EEG)(FDR > 0.2, mean normalized expression over both species >5). The group of orthologous genes was clustered by principal component analysis. The DEG and EEG group were compared on gene count level in the three sub-categories molecular function, cellular component, and biological process. These orthologous genes should provide a classification of evolutionary conservation patterns. Furthermore, ortholog genes , annotated to one of three selected gene ontologies were examined for their chromosomal identity between the species in a circos plot. EEG and DEG were seperated to investiagte positions similarities and variations and if these were correlating with genomic positions.

Venn diagrams were prepared using the R package VennDiagram 1.6.20 (33). Bioconductor packages ComplexHeatmap 2.6.2 (34) and Circlize 0.4.11 (35) were used to create the heatmaps. Correlations were performed by corrplot 0.84 package (36). GO term bar plots were printed using ggplot2 3.3.2 package. Principal component analysis and plots were created by PCAtools 2.2.0 (37) and complex boxplot with either ggplot2 3.3.2 or ggpubr 0.4.0 packages (38,39). Finally, circos plots were created with OmicCircos 1.2.0 (40).

3. Results

The presented study covered multiple comparison levels to provide a general overview of physiological processes in different tissues and species at the seedling stage under a short-day photoperiod regime. On the first level, root and shoot meristems within the species were tested against each other to uncover tissue-related gene expression variations. Transcriptome analysis using MACE revealed 7.9

160 million reads in barley root apices, of which 5.5 million reads were aligned across the barley genome.
161 Among the mapped reads, 4.7 million reads were aligned to barley annotated genes. More transcripts
162 (10.5 million) were found in the barley shoot, of which 5.9 million reads were mapped and aligned with
163 barley annotated genes (Figure S2A). In tomato root and shoot apices, around 12.4 and 7.9 million
164 reads were identified, of which 7.1 and 5.5 million reads were mapped to annotated genes,
165 respectively (Figure S2B). Across tissues and species, the three replicates indicated high similarities
166 (Figure S3). Pearson correlations of the normalized gene expression between the replicates ranged
167 from 0.97 to 1.00. The calculated p-value between the replications for all genes supports the
168 similarities of replicates observed in the correlation analysis ($r > 0.99$).

169 ## Barley tissue comparison

170 We detected 16,842 of 39,811 genes (42%) to be expressed in both barley tissues (Figure 1A), from
171 which 1,918 were significantly upregulated in the shoot and 2,214 in the root meristem (Figure 1B, 1C).
172 Additionally, 1,085 genes have been expressed in the root only, while 1,533 genes show expression
173 only in shoot tissue (Figure 1A, Suppl. Table 1). By performing a gene ontology enrichment based on
174 the gene cluster occurrences in the overexpressed genes, 51 significant ontology classes were
175 observed (Figure S4, Suppl. Table 2). The most significant GO terms were identified for cell wall
176 organization, oxidation-reduction processes, and heme-binding ($p < 0.0001$). On a lower but still
177 significant level of probability ($p < 0.05$), transcription factor activities and metabolic process
178 regulations have been observed to vary between the root and shoot. These observations were further
179 quantified by an expression level analysis of GO terms (Suppl. Table 3). Ten significantly different
180 ontologies were detected, where five of these show an up-regulation in root tissue (Figure 1D). Three
181 of these genes are related to the transport of nutrients (ammonium transport, phosphate transport,
182 transmembrane transporter), while one is related to the energy process (sucrose alpha-glucosidase)
183 and the last and strongest associated with oxidative stress response (oxidoreductase activity). Another
184 family of oxidoreductase genes is significantly upregulated in the shoot meristem, but the absolute
185 expression is much lower than in the root tissue.

Furthermore, two other oxidative response classes were observed (cyclase activity, antioxidation activity). Besides these three stress-responsive ontology classes, the photosystem I reaction center and glycerol kinase activity were overexpressed. Thus, concluding the observations made on the barley tissue comparison level, a sink source pattern can be observed with the additional oxidative stress response.

Tomato tissue comparison

In tomato, 20,297 of 33,812 genes (60%) were expressed in both tissues, from which 1,537 were upregulated in the shoot and 1,874 upregulated in the root meristem. Additionally, 1,835 genes have shown expression in the root, while 1,362 genes are only expressed in the shoot tissue (Figure 2A-C, Suppl. Table 4). Gene ontology clustering based on the DEG resulted in 63 significant variations between root and shoot tissue (Figure S5, Suppl. Table 5). The most pronounced variation was noticed for stress response, cell wall organization, metabolic processes, transcription factor binding, transporter activity, and photosystem I. By comparing the gene expression level of root and shoot tissue against each other on the GO term level, 27 significantly different classes have been observed (Suppl. Table 6). Eleven of these (41%) are overexpressed in the root compared to the shoot tissue, while 16 are overexpressed in the shoot tissue. Most of the root-related GO terms can be classified in the functional groups of transporting (transmembrane transporter), reservoir activity (nutrient reservoir activity, beta-carotene monooxidase activity, anthocyanin glucosyltransferase), nutrient uptake (Nicotianamine biosynthesis), and elongation (apoplast, gibberellin oxidase). For the shoot, few superordinate classes were identified, which are growth (elongation), photosynthetic activity (protochlorophyllide reductase, photolyase, rubisco, photosystem I and II, chlorophyll-binding, extrinsic to membrane), oxidative response (Flavonoid biosynthesis, oxidoreductase, formamidase activity), developmental activities (indole acid carboxyl transferase) and energy transformation (acetyl-CoA reductase, glyoxylate reductase). The highest overall expression can be reported for photosynthesis-related processes directly linked to photosystems I and II (Figure 2D).

Comparison of barley and tomato development

While the roots showed equal functional activity between barley and tomato gene ontologies, the shoot tissues varied in photosynthetic activity levels. Remarkably, the oxidoreductase activity (acting on CH-CH group donors) was found to be overexpressed in tomato shoot tissue and barley shoot tissue, while lowly expressed in root tissues (Figure 1D & 2D). Compared to the barley GO clustering, 2.7 times more differentially expressed GO terms were observed. The reduced expressional activity in barley tissues resulted in a lower tissue-specific differentiation level (Figure 3A). The principal component analysis revealed variations between species on gene ontology expression level, presented by the first component. This first component explains more than 70% of the entire variation. The second component explains 17%, related to the tissue-specific variation. Generally, a more pronounced differentiation of the tomato tissues compared to the barley tissues was observed. Based on the LFC comparison between barley and tomato, 12 GO terms were identified to be significantly different between the two species (Figure 3B).

Generally, three major groups can be clustered from the direct GO expression comparison. The first group is photosynthetic activity (Photosystem II, Chlorophyll binding) (Figure S7C& S6C). The activity was highest in tomato shoot tissue, while little expression was detected in barley. In contrast, the photosystem I indicated similar expression patterns in barley and tomato (Figure 1D & 2D). The second group was related to stress response on the cellular level, including response to wounding, peroxidase activity, and defense response. While the peroxidase activity differed between the species on $p < 6.5e^{-10}$, the intraspecies tissue variation was $p < 0.001$ (Figure 3B). Besides the peroxidase activity (Figure S6B), chlorophyll-binding (Figure S6C), defense response (Figure S7E), and the response to wounding (Figure S7I) were discovered for this group. Generally, the expression magnitude for the GO terms was higher in root tissues, with an overall higher expression in tomato. A higher level of expression in tomato was also observed for the other two stress-responsive GO terms (Figure S7E & I). Finally, the biggest group was related to respiratory and developmental processes. NADH dehydrogenase, 4 iron 4 sulfur cluster binding, and proton-transporting ATPase activity might be associated with respiratory

functions. The ribosomal constitution, protein binding, and calcium-binding appear to be related to developmental processes. No variation between the tomato tissues was observed for the developmental processes, but an increased expression compared to the barley tissues (Figure S7A, D & G). The same holds for the respiratory GO terms. No variation between tissues of the same species was observed. Nevertheless, significant overexpression of genes in the tomato tissues was detected compared to the barley tissue (Figure S6A, S6D & S7H).

Subsequently, we wanted to compare the expression of *Cry1* and *Cry2* in both species and tissues. These cryptochromes were reported to mediate the photoperiodic control of flowering, entrainment of the circadian clock, cotyledon opening and expansion, anthocyanin accumulation, and root growth (41). The *blastn* of Hv-CRY1a/b and Hv-CRY2 sequences, derived from (42), revealed *HORVU6Hr1G049950* (Hv-CRY1) and *HORVU6Hr1G058740* (Hv-CRY2) as single hits. We compared the expression of Hv-CRY1/2 in root and shoot to the expression of ortholog tomato *Cry1* and *Cry2* genes **(Figure 4).** Locus information of tomato orthologs was derived from (41). While we did not observe variations in the gene expression of *Cry2* in shoot tissues between tomato and barley, *Cry1* revealed 2.3 times higher gene expression in tomato compared to barley shoot. The root tissue expression of *Cry1* and *Cry2* revealed a 1.95 and 2.87 times overexpression in the barley root tissue compared to tomato, respectively.

Conserved protein sequences and transcription patterns

Five hundred nineteen orthologous genes were identified based on their protein structure homology. These were used to estimate the magnitude of conservation in the expression level (Figure 4A, Suppl. Table 7). This 1-to-1 sequence similarity relationship indicates that these respective barley and tomato genes were more closely related than to any other genes.

A principal component clustering of these genes exposed the higher transcriptional relation tissue-wise in this set of orthologues (Figure 5A). Compared to the collection of GO expression of all genes in figure 3A, the tissues show evidence of increased transcriptional conservation in the group of

orthologous genes. While the first component separates the root tissue, the shoot tissues are separated by the second component. The clustering of these orthologues in DEG and EEG results in two unequally sized groups. Based on a threshold of at least five reads in either set, 94 and 91 DEG were identified, comparing the species tissue-wise for root and shoot, respectively. The majority of these genes were not, or only marginally expressed in barley. With a minimal expression threshold of five reads in both species, the number of DEG was reduced to 12 and 14 in root and shoot, respectively (Figure 5B). Six of these genes were found in both tissues. These include endopeptidase activity, proteolysis, structural constituent of ribosome, SNAP receptor activity, and response to stress and oxidation-reduction. These genes have a significant overexpression in the tomato tissues in common, with an average LFC value of ten.

The other group of EEGs was almost four times bigger (Figure 5B). Forty-one EEGs have been identified in the root gene expression, while forty-five EEGs were detected in the shoot comparison. Seven of these were found in both tissues, including transcription coactivator activity, clathrin binding, hydrolase activity, protein binding, metabolic processes, and two endonuclease activity genes. The average expression of these genes was 298 normalized fragments, indicating an overall high expression level. For the EEG in the root, four were annotated as transcription factors, ten were related to protein binding, 14 were identified as enzymes, two were related to oxidation reactions, and four were identified as endonuclease enzymes. In shoot-related EEG observed genes, 14 enzymes were identified. Nine of these were described as transcription factors, five protein-binding-related genes, seven genes with oxidation background, and three endopeptidases. Several genes were annotated to more than one function.

High expressional conservation between the species was observed when clustered to biological processes, cellular components, and molecular function (Figure 5B). Especially the count of EEG in the molecular function group is 4.3 and 5.4 times higher than the DEG for shoot and root, respectively. The

other two groups show lower representation in both groups, which results in no variation between DEG and EEG.

Ultimately, we mapped the ortholog genes and compared their genomic position between the species. As the three groups transport, translation, and photosynthesis have caught the most interest, we compared the genomic loci between tomato and barley for DEG (Figure 5C), and EEG (Figure 5D) expressed ortholog genes. Three photosynthesis, one transport, and two translation-related genes were identified among the DEG group. Analog, one photosynthesis, six transport, and five translation-related ortholog genes were observed for the EEG group. The comparison of the genomic loci revealed a hotspot on barley's chromosome 5H, where five of six DEG ortholog genes were located. Besides, three EEG transport-related genes were found on 5H. Contrasting to barley, the distribution of the DEG and EEG ortholog genes did not indicate any clustering on the tomato genome.

In conclusion, the orthologues' significant variation in expression is related to a void barley root and shoot gene expression at the seedling stage. For the set of genes showing expression in both tissues, the majority is described by the group of molecular functions. Most of these genes indicated a similar expression.

4. Discussion

The functional analysis of these two divergent species was performed after a cultivation period of ten days, described by a photoperiod of 8h. While modern tomato varieties are day-length neutral (43), barley, as facultative long-day species (44), depends on long photoperiods to flower. Regarding this habit, short day-length was also observed to suppress growth and development in barley at the seedling stage (45). Although the photoperiodic habit of species is generally determined, the day length type depends on the presents or expression level of specific candidate genes and, therefore, is interchangeable (43). Furthermore, mutation breeding has created barley varieties with day-length neutral habits, indicating the potential to change the photoperiodic sensitivity (44).

This study aimed to identify significant variations and similarities of physiological development in early seedling stages between a day-length neutral tomato variety and a long-day barley variety. Therefore, root apices, comprising root meristem and root elongation zone of barley and tomato, were precisely harvested under a dissecting microscope. Likewise, shoot meristems comprising two emerging leaf primordia were gathered in both species. To homogenize the sampling process, we cut exactly 50 root and shoot apices (as technical replicates) and pooled them in each biological replicate. The primary reason behind this sampling strategy was to target development-related genes and ensure the reproducibility of transcript data. Our data showed very highly similar gene expression among the individual biological replicates in each tissue in both species, suggesting that the adopted sampling strategy was appropriate (Figure S2, S3).

We used massive cDNA Ends (MACE) analysis instead of whole transcriptome sequencing by standard RNAseq approaches. MACE was preferred over RNAseq for two reasons. First, the bias of gene length should be avoided. While the gene length variation does not matter too much in intraspecies transcriptome analysis, the comparison between species results in gene length expression bias. Both the orthologue genes and the gene ontology comparison on expression level could be biased by the gene length-related expression. Although the expression could have been corrected by the gene length, only sequencing the 3' single end of the gene gives higher confidence in the processed approach. Second, PCR duplicates are reduced due to the applied TrueQuant approach while sequencing. This should ensure minimal PCR bias during transcriptome sequencing. Ideally, each template molecule can be identified by its unique TrueQuant adapter sequence. Based on this, PCR copies can be determined and eliminated from the dataset, and uneven amplification and artifacts generated during the PCR amplification can be eliminated. Nevertheless, MACE also has some relevant disadvantages, like the comparably short read length and the sequencing on the 3' end. These two might have caused the significant loss of fragments throughout the alignment, filtering, and annotation process. As previously reported, inaccurate gene annotations might result in failed read annotations for those fragments with a start position beyond the annotated gene start (46). This becomes a more

336 relevant issue the shorter the reads are. Besides, the precise alignment of very short single-end reads
337 is challenging. Maybe this was the other reason for the high number of unaligned reads.
338
339 In the functional analysis, the intraspecies comparison revealed a generally lower expression of genes
340 in barley tissues than tomato. While only about 48% of all genes were expressed in barley, almost 73%
341 of all genes have shown evidence of activity in tomato. The higher number of expressed genes is also
342 represented by a higher relative number of DEG in Tomato compared to barley (Figure 2). This can be
343 seen as a first indication of lower differentiation activity in barley tissues. A GO enrichment, based on
344 the occurrences of DEG, revealed twelve more variant terms in the tomato root to shoot comparison
345 than for the barley tissues (Figure 3). Similarities were found for the terms cell wall organization,
346 metabolic processes, and transcription factor binding. In addition, variations were observed for stress
347 response and photosynthetic activity, which showed variance in the tomato tissues, but not between
348 the barley tissues.
349 Based on an expression value comparison of root to shoot tissues, particular GO variations between
350 the species were observed. Barley root tissue-specific ontologies were nutrient transportation,
351 respirational aspects, and oxidative stress response. In tomato, gene overexpression in roots was
352 found for nutrient uptake, transport, and storage groups. Additionally, elongational processes can be
353 observed, indicating growth processes in the root tissue. Comparing the shoot level, both species have
354 an overexpression in oxidative response classes and the photosystem I activity in common. Besides
355 these, six additional GO classes related to the photosynthetic activity are overexpressed in the tomato
356 shoot tissue. Overexpression of photosynthetic genes in the shoot is not unexpected, but the missing
357 overexpression in barley tissue makes it remarkable. Developmental gene ontologies and energy
358 transforming processes indicated that tomato shoot tissue was associated with superior energy
359 production under short-term light conditions compared to barley shoot tissue. Nevertheless, this
360 variation might also be caused by the lower seed weight of tomato compared to barley. This might

force tomato seedlings to overweight the energy production and photosynthesis gene expression compared to barley. Overall, there were 2.7 times more gene ontologies found in tomato to vary between root and shoot tissues. This might indicate higher tissue specificity, probably associated with a more pronounced developmental variation under the given light regime.

The following comparison level supported the GO variations' higher physiological and metabolic activity in tomato tissue. Therefore, the LFC variation between root and shoot tissues on the intraspecies level was compared between the species. Two photosynthesis-related GO terms were highly expressed in the tomato shoot (Figure 2), but not in the barley shoot (Figure 1). Especially interesting is the low expression level of photosystem II-related genes in barley shoot tissue. The photosystems cover a different range of light absorbance (680nm, 720nm), which leads to a reduced energy transformation from less energetic light, due to the reduced activity of the photosystem II (47).

Furthermore, the activity of photosystem II is reported to require more light than photosystem I (48). Evolutionary variant extrinsic proteins might have a crucial effect on the structure and function of the photosystem II (49). The reduced photosynthetic activity is framed in an overall reduced physiological activity in barley tissues. The reduced physiological activity was assumed based on the structural constituent of ribosomes, protein binding, NADPH dehydrogenase, or proton-transporting ATPase activity. The structural constituent of ribosomes plays a crucial role in regulating gene expression (50–52). The count of protein-binding related genes has been observed to be one of the most expressed groups, which might be related to tissue differentiation processes (53) or the regulation of plant developmental processes by protein-protein interactions (54). NADPH dehydrogenase, relevant in the respiratory chain (55,56), was more active in tomato tissues. The activity of NADPH dehydrogenases was reported to be dependent on Ca^{2+} (57). Calcium has several roles in plant development (58), and we observed the calcium ion binding expression also being higher in tomato tissues. This might indicate that a reduced calcium ion binding results in reduced activity of the NADPH dehydrogenases and, ultimately, reduced development and differentiation in barley tissues. The PCA shows a higher tissue

386 distinction in tomato (Figure 3A), indicating a more pronounced developmental variation under the
387 given light regime. The observed higher expression of stress-responsive genes in tomato tissues might
388 be associated with unfavorable photoperiodic cycle conditions induced injuries, as described by
389 Hillman (1956)(59).

390 The candidate genes *Cry1* and *Cry2* were selected as target genes, as these were described to have a
391 relevant impact on tissue differentiation. Furthermore, the expression pattern was observed to change
392 over time (7). From the observation made in our experiment, one could conclude that tomato
393 promotes shoot over root development (Figure 4). Contrasting, barley promotes the root growth
394 overshoot development. But, as our experiment lacked a barley expression profile in a long-day light
395 regime, we compared the observed *Cry1* and *Cry2* expression patterns to literature-obtained
396 expression data. By this comparison, we aimed to answer whether the lower expression of *Cry1* in
397 barley was associated with the species or the 8h light regime. Compared to the expression profile of
398 Morex seedlings, derived by (60), *Cry1* was 2.9 times higher expressed in Morex under 16h light regime
399 (external source) than Scarlett under 8h (Figure S8). Similarly, *Cry2* was 2.14 times higher expressed in
400 Morex compared to Scarlett. As these are two different genotypes and the sampling time point
401 marginally differs, observed variations could be due to genotypic or time variations. Nevertheless, the
402 expression variation between the environments for barley was highly significant, and the expression
403 of Morex 16h was even beyond the level observed in tomato. Therefore, it could indicate that *Cry1*
404 and *Cry2* alleles in Scarlett would be higher expressed than tomato orthologs under a 16h light regime.

405

406 Additionally, the expression conservation level between these two species was investigated by
407 comparing orthologous genes. The hypothesis of the structural relation of genes leading to a higher
408 level of equal expression can be confirmed. In the group of molecular functions, five times more genes
409 showed equivalent expression compared to differential expression (Figure 5). The other two groups
410 were shallowly covered, indicating that functional conservation beyond species levels is more likely in

411 basic molecular functions. This statement is supported by the genes found to be EEG related to core
412 functionalities, like enzyme activity and translational processes. All DEG genes have shown
413 overexpression in tomato tissue, while most of these genes were not expressed in barley. This might
414 change with a different light regime and might be another indicator for delayed and reduced
415 physiological activity under short daylight conditions.

416 Comparing physical positions of ortholog genes annotated to photosynthesis, transport, and
417 translation-related functions did not reveal that ortholog genes, similar in expression patterns, are not
418 clustered by chromosomes. Similar results were observed for EEG, indicating that these two species
419 are different in their genomic construction.

420 5. Conclusion

421 Applying a short photoperiod regime resulted in gene expression variations between tissues and
422 species. The photoperiod is a relevant regulator for photosynthetic activity physiological and
423 morphological differentiation for photoperiod sensitive species like barley. As early sowing dates of
424 spring-type crops result from climate change, the reduced growth under shorter day length conditions
425 can indicate undesired lower productivity in unadapted varieties. Breeding of new, less photoperiod
426 sensitive barley varieties might overcome delayed development and differentiation. Growth
427 suspension by short photoperiod could benefit from genetic adjustments to avoid the coincidence of
428 flowering and spring drought. This could retain high yields in rainfed crops by drought avoidance
429 strategies through early root development.

430 Author's contribution

431 AAN and JL conceptualize the research. MS, AAN, BM, LV, HS, OBC analyze the data. MS, AAN and LV
432 have written the manuscript.

433 Competing interests

434 The authors declare no competing interests.

Acknowledgements

We are grateful to Mrs. A. Bungartz for her help in sample preparation. Special thanks to Mrs. Anna Vlasova for her valuable suggestion in data analysis and to Mr. Md. Kamruzzaman for reading the manuscript.

References

1. Wolfe KH, Gouy M, Yang YW, Sharp PM, Li WH. Date of the monocot-dicot divergence estimated from chloroplast DNA sequence data. Proc Natl Acad Sci U S A [Internet]. 1989 Aug 1 [cited 2020 Dec 21];86(16):6201–5. Available from: https://www.pnas.org/content/86/16/6201
2. Naz AA, Raman S, Martinez CC, Sinha NR, Schmitz G, Theres K. Trifoliate encodes an MYB transcription factor that modulates leaf and shoot architecture in tomato. Proc Natl Acad Sci U S A [Internet]. 2013 Feb 5 [cited 2020 Dec 21];110(6):2401–6. Available from: /pmc/articles/PMC3568312/?report=abstract
3. Nori H, Moot DJ, Black AD. Leaf appearance of annual clovers responds to photoperiod at emergence. Eur J Agron [Internet]. 2016;72:99–106. Available from: http://dx.doi.org/10.1016/j.eja.2015.10.004
4. Hotsonyame GK, Hunt LA. Sowing date and photoperiod effects on leaf appearance in field-grown wheat. Can J Plant Sci. 1997;77(1):23–31.
5. Perrotta G, Yahoubyan G, Nebuloso E, Renzi L, Giuliano G. Tomato and barley contain duplicated copies of cryptochrome 1. Plant, Cell Environ. 2001;24(9):991–8.
6. Wang X, Wang Q, Nguyen P, Lin C. Cryptochrome-mediated light responses in plants. Enzymes. 2014;35:167–89.
7. D'Amico-Damião V, dos Santos JC, Girotto NC, Carvalho RF. Cryptochrome 1a influences source-sink partitioning during different stages of growth in tomato. Theor Exp Plant Physiol. 2019;31(2):295–302.
8. Ko D, Helariutta Y. Shoot–Root Communication in Flowering Plants. Vol. 27, Current Biology. Cell Press; 2017. p. R973–8.
9. Glanz-Idan N, Tarkowski P, Turečková V, Wolf S. Root-shoot communication in tomato plants: Cytokinin as a signal molecule modulating leaf photosynthetic activity. Lunn J, editor. J Exp Bot [Internet]. 2020 Jan 1 [cited 2020 Dec 21];71(1):247–57. Available from: https://academic.oup.com/jxb/article/71/1/247/5556948
10. Borràs-Gelonch G, Slafer GA, Casas AM, van Eeuwijk F, Romagosa I. Genetic control

of pre-heading phases and other traits related to development in a double-haploid barley (Hordeum vulgare L.) population. F Crop Res. 2010;119(1):36–47.

11. Alqudah AM, Sharma R, Pasam RK, Graner A, Kilian B, Schnurbusch T. Genetic dissection of photoperiod response based on gwas of pre-anthesis phase duration in spring barley. PLoS One. 2014 Nov 24;9(11).

12. Soyk S, Müller NA, Park SJ, Schmalenbach I, Jiang K, Hayama R, et al. Variation in the flowering gene SELF PRUNING 5G promotes day-neutrality and early yield in tomato. Nat Genet. 2017;49(1):162–8.

13. Slafer GA, Abeledo LG, Miralles DJ, Gonzalez FG, Whitechurch EM. Photoperiod sensitivity during stem elongation as an avenue to raise potential yield in wheat. In: Euphytica. 2001. p. 191–7.

14. Hunter RB, Tollenaar M, Breuer CM. Effects of photoperiod and temperature on vegetative and reproductive growth of a maize (zea mays) hybrid. Can J Plant Sci [Internet]. 1977 Oct 1 [cited 2020 Dec 20];57(4):1127–33. Available from: https://cdnsciencepub.com/doi/abs/10.4141/cjps77-167

15. Keeling CD, Chin JFS, Whorf TP. Increased activity of northern vegetation infered from atmospheric CO2 measurements. Nature. 1996;382:146–9.

16. Linderholm HW. Growing season changes in the last century. Vol. 137, Agricultural and Forest Meteorology. Elsevier; 2006. p. 1–14.

17. Körner C, Basler D. Phenology under global warming [Internet]. Vol. 327, Science. American Association for the Advancement of Science; 2010 [cited 2020 Dec 20]. p. 1461–2. Available from: www.sciencemag.orgSCIENCEVOL

18. Bauerle WL, Oren R, Way DA, Qian SS, Stoy PC, Thornton PE, et al. Photoperiodic regulation of the seasonal pattern of photosynthetic capacity and the implications for carbon cycling. Proc Natl Acad Sci U S A [Internet]. 2012 May 29 [cited 2020 Dec 20];109(22):8612–7. Available from: www.pnas.org/cgi/doi/10.1073/pnas.1119131109

19. Zawada AM, Rogacev KS, Müller S, Rotter B, Winter P, Fliser D, et al. Massive analysis of cDNA Ends (MACE) and miRNA expression profiling identifies proatherogenic pathways in chronic kidney disease. Epigenetics [Internet]. 2014 Jan [cited 2020 Feb 10];9(1):161–72. Available from: http://www.ncbi.nlm.nih.gov/pubmed/24184689

20. Bolger AM, Lohse M, Usadel B. Trimmomatic: A flexible trimmer for Illumina sequence data. Bioinformatics [Internet]. 2014 Aug 1 [cited 2020 Feb 12];30(15):2114–20. Available from: https://academic.oup.com/bioinformatics/article-lookup/doi/10.1093/bioinformatics/btu170

21. Cunningham F, Achuthan P, Akanni W, Allen J, Amode MR, Armean IM, et al. Ensembl 2019. Nucleic Acids Res [Internet]. 2019 Jan 8 [cited 2020 Sep

8];47(D1):D745–51. Available from: http://test-metadata.ensembl.org/

22. Li H, Durbin R. Fast and accurate short read alignment with Burrows-Wheeler transform. Bioinformatics [Internet]. 2009 [cited 2019 Nov 15];25(14):1754–60. Available from: http://massgenomics.org/2009/12/making-the-leap-maq-to-bwa.html

23. Li H, Handsaker B, Wysoker A, Fennell T, Ruan J, Homer N, et al. The Sequence Alignment/Map format and SAMtools. Bioinformatics [Internet]. 2009 Aug 15 [cited 2020 Feb 8];25(16):2078–9. Available from: https://academic.oup.com/bioinformatics/article-lookup/doi/10.1093/bioinformatics/btp352

24. Parekh S, Ziegenhain C, Vieth B, Enard W, Hellmann I. The impact of amplification on differential expression analyses by RNA-seq. Sci Rep [Internet]. 2016 May 9 [cited 2020 Dec 20];6(1):1–11. Available from: www.nature.com/scientificreports

25. Liao Y, Smyth GK, Shi W. FeatureCounts: An efficient general purpose program for assigning sequence reads to genomic features. Bioinformatics [Internet]. 2014 Apr 1 [cited 2020 Dec 20];30(7):923–30. Available from: https://pubmed.ncbi.nlm.nih.gov/24227677/

26. R Core Team. R: A Language and Environment for Statistical Computing [Internet]. Vienna, Austria; 2020. Available from: https://www.r-project.org/

27. Bezanson J, Edelman A, Karpinski S, Shah VB. Julia: A fresh approach to numerical computing. SIAM Rev. 2017;59(1):65–98.

28. McCarthy DJ, Chen Y, Smyth GK. Differential expression analysis of multifactor RNA-Seq experiments with respect to biological variation. Nucleic Acids Res. 2012;40(10):4288–97.

29. Robinson MD, McCarthy DJ, Smyth GK. edgeR: A Bioconductor package for differential expression analysis of digital gene expression data. Bioinformatics [Internet]. 2009;26(1):139–40. Available from: http://bioconductor.org

30. Tian T, Liu Y, Yan H, You Q, Yi X, Du Z, et al. AgriGO v2.0: A GO analysis toolkit for the agricultural community, 2017 update. Nucleic Acids Res [Internet]. 2017 Jul 3 [cited 2020 Sep 30];45(W1):W122–9. Available from: /pmc/articles/PMC5793732/?report=abstract

31. Li L, Stoeckert CJ, Roos DS. OrthoMCL: Identification of ortholog groups for eukaryotic genomes. Genome Res [Internet]. 2003 Sep 1 [cited 2020 Dec 20];13(9):2178–89. Available from: /pmc/articles/PMC403725/?report=abstract

32. Altschul SF, Gish W, Miller W, Myers EW, Lipman DJ. Basic local alignment search tool. J Mol Biol [Internet]. 1990 [cited 2020 Oct 24];215(3):403–10. Available from: https://pubmed.ncbi.nlm.nih.gov/2231712/

33. Chen H. VennDiagram: Generate High-Resolution Venn and Euler Plots [Internet].

2018. Available from: https://cran.r-project.org/package=VennDiagram

34. Gu Z, Eils R, Schlesner M. Complex heatmaps reveal patterns and correlations in multidimensional genomic data. Bioinformatics. 2016;

35. Gu Z, Gu L, Eils R, Schlesner M, Brors B. circlize implements and enhances circular visualization in R. Bioinformatics. 2014;30(19):2811–2.

36. Wei T, Simko V. R package "corrplot": Visualization of a Correlation Matrix [Internet]. 2017. Available from: https://github.com/taiyun/corrplot

37. Blighe K. PCAtools: PCAtools: Everything Principal Components Analysis [Internet]. 2019. Available from: https://github.com/kevinblighe/PCAtools

38. Kassambara A.' ggpubr': "ggplot2" Based Publication Ready Plots. R Packag version 025. 2020;

39. Wickham H. ggplot2: Elegant Graphics for Data Analysis [Internet]. Springer-Verlag New York; 2016. Available from: https://ggplot2.tidyverse.org

40. Hu Y, Yan C, Hsu CH, Chen QR, Niu K, Komatsoulis GA, et al. Omiccircos: A simple-to-use R package for the circular visualization of multidimensional Omics data. Cancer Inform [Internet]. 2014 Jan 16 [cited 2022 Mar 2];13:13–20. Available from: https://pubmed.ncbi.nlm.nih.gov/24526832/

41. Fantini E, Sulli M, Zhang L, Aprea G, Jiménez-Gómez JM, Bendahmane A, et al. Pivotal Roles of Cryptochromes 1a and 2 in Tomato Development and Physiology. Plant Physiol [Internet]. 2019 Feb 1 [cited 2022 Mar 2];179(2):732. Available from: /pmc/articles/PMC6426409/

42. Barrero JM, Downie AB, Xu Q, Gubler F. A role for barley CRYPTOCHROME1 in light regulation of grain dormancy and germination. Plant Cell [Internet]. 2014 Apr 23 [cited 2022 Mar 2];26(3):1094–104. Available from: https://academic.oup.com/plcell/article/26/3/1094/6099892

43. Mizoguchi T, Niinuma K, Yoshida R. Day-neutral response of photoperiodic flowering in tomatoes: Possible implications based on recent molecular genetics of Arabidopsis and rice. Plant Biotechnol. 2007;24(1):83–6.

44. Hanumappa M, Pratt LH, Cordonnier-Pratt MM, Deitzer GF. A Photoperiod-Insensitive Barley Line Contains a Light-Labile Phytochrome B. Plant Physiol [Internet]. 1999 [cited 2021 Dec 8];119(3):1033. Available from: /pmc/articles/PMC32084/

45. HAY RKM. The influence of photoperiod on the dry matter production of grasses and cereals [Internet]. Vol. 116, New Phytologist. John Wiley & Sons, Ltd; 1990 [cited 2021 Dec 8]. p. 233–54. Available from: https://onlinelibrary.wiley.com/doi/full/10.1111/j.1469-8137.1990.tb04711.x

578 46. Duarte-Delgado D, Dadshani S, Schoof H, Oyiga BC, Schneider M, Mathew B, et al.
579 Transcriptome profiling at osmotic and ionic phases of salt stress response in bread
580 wheat uncovers trait-specific candidate genes. BMC Plant Biol 2020 201 [Internet].
581 2020 Sep 16 [cited 2021 Sep 15];20(1):1–18. Available from:
582 https://bmcplantbiol.biomedcentral.com/articles/10.1186/s12870-020-02616-9

583 47. Barber J. Photosynthetic energy conversion: Natural and artificial. Chem Soc Rev
584 [Internet]. 2009 Dec 16 [cited 2020 Dec 22];38(1):185–96. Available from:
585 https://pubs.rsc.org/en/content/articlehtml/2009/cs/b802262n

586 48. Scholthof K-BG. The Molecular Life of Plants . By Russell Jones, Helen Ougham,
587 Howard Thomas, and Susan Waaland. Hoboken (New Jersey): Wiley-Blackwell.
588 $179.95 (hardcover); $99.95 (paper). xxiv + 742 p.; ill.; index. ISBN: 978-0-470-
589 87011-2 (hc); 978-0-470-87012-9 (pb). . Q Rev Biol [Internet]. 2014 Jun 19 [cited
590 2020 Dec 21];89(2):185–6. Available from:
591 https://www.journals.uchicago.edu/doi/abs/10.1086/676086

592 49. Ifuku K, Noguchi T. Structural coupling of extrinsic proteins with the oxygen-evolving
593 center in photosystem II. Front Plant Sci [Internet]. 2016 Feb 5 [cited 2020 Dec
594 22];7(FEB2016):84. Available from:
595 http://journal.frontiersin.org/Article/10.3389/fpls.2016.00084/abstract

596 50. Berisio R, Schluenzen F, Harms J, Bashan A, Auerbach T, Baram D, et al. Structural
597 insight into the role of the ribosomal tunnel in cellular regulation. Nat Struct Biol
598 [Internet]. 2003 May 1 [cited 2020 Dec 22];10(5):366–70. Available from:
599 http://www.nature.com/naturestructuralbiology

600 51. Graifer D, Malygin A, Zharkov DO, Karpova G. Eukaryotic ribosomal protein S3: A
601 constituent of translational machinery and an extraribosomal player in various cellular
602 processes. Vol. 99, Biochimie. Elsevier; 2014. p. 8–18.

603 52. Bhavsar RB, Makley LN, Tsonis PA. The other lives of ribosomal proteins. [Internet].
604 Vol. 4, Human genomics. BioMed Central; 2010 [cited 2020 Dec 22]. p. 327–44.
605 Available from: https://link.springer.com/articles/10.1186/1479-7364-4-5-327

606 53. Musseau C, Jorly J, Gadin S, Sørensen I, Deborde C, Bernillon S, et al. The tomato
607 guanylate-binding protein SlGBP1 enables fruit tissue differentiation by maintaining
608 endopolyploid cells in a non-proliferative state. Plant Cell [Internet]. 2020 [cited 2020
609 Dec 22];32(10):3188–205. Available from:
610 www.plantcell.org/cgi/doi/10.1105/tpc.20.00245

611 54. Struk S, Jacobs A, Sánchez Martín-Fontecha E, Gevaert K, Cubas P, Goormachtig S.
612 Exploring the protein–protein interaction landscape in plants [Internet]. Vol. 42, Plant
613 Cell and Environment. Blackwell Publishing Ltd; 2019 [cited 2020 Dec 22]. p. 387–
614 409. Available from: http://doi.wiley.com/10.1111/pce.13433

615 55. Michalecka AM, Agius SC, Møller IM, Rasmusson AG. Identification of a

mitochondrial external NADPH dehydrogenase by overexpression in transgenic *Nicotiana sylvestris*. Plant J [Internet]. 2004 Feb 9 [cited 2020 Dec 22];37(3):415–25. Available from: https://onlinelibrary.wiley.com/doi/abs/10.1046/j.1365-313X.2003.01970.x

56. Melo AMP, Duarte M, Møller IM, Prokisch H, Dolan PL, Pinto L, et al. The External Calcium-dependent NADPH Dehydrogenase from Neurospora crassa Mitochondria. J Biol Chem [Internet]. 2001 Feb 9 [cited 2020 Dec 22];276(6):3947–51. Available from: http://www.jbc.org/

57. Rasmusson AG, Moller IM. Effect of calcium ions and inhibitors on internal NAD(P)H dehydrogenases in plant mitochondria. Eur J Biochem [Internet]. 1991 Dec 1 [cited 2020 Dec 22];202(2):617–23. Available from: http://doi.wiley.com/10.1111/j.1432-1033.1991.tb16415.x

58. Hepler PK, Wayne RO. Calcium and Plant Development. Annu Rev Plant Physiol [Internet]. 1985 [cited 2020 Dec 22];36(1):397–439. Available from: www.annualreviews.org

59. Hillman WS. Injury of Tomato Plants by Continuous Light and Unfavorable Photoperiodic Cycles. Am J Bot. 1956 Feb;43(2):89.

60. Liu H, Li G, Yang X, Kuijer HNJ, Liang W, Zhang D. Transcriptome profiling reveals phase-specific gene expression in the developing barley inflorescence. Crop J. 2020 Feb 1;8(1):71–86.

Legend of Figures

Figure 1. Overview of root to shoot tissue expression in barley. A – count of expressed genes in shoot tissue only, both tissues and root tissue only. B – volcano plot of differentially expressed genes, visualizing the Bonferroni adjusted -log10 probability value against the log2 fold change. Blue dots indicate significantly upregulated genes in root tissue; red indicates the same for shoot tissue. C – heatmap of all DEG for the root and shoot tissue. The mean expression value over the three replicates is shown on a log10 transformation. D – differentially expressed gene ontologies. The exterior color of the bar splits root (blue) from the shoot (green), the p-value is indicated by the bar fill. The bars represent the average normalized expression value for the GO terms, based on all genes related to the GO term.

Figure 2. Overview of root to shoot tissue expression in tomato. A – count of expressed genes in shoot tissue only, both tissues and root tissue only. B – volcano plot of differentially expressed genes, visualizing the Bonferroni adjusted -log10 probability value against the log2 fold change. Blue dots indicate significantly upregulated genes in root tissue; red indicates the same for shoot tissue. C – heatmap of all DEG for the root and shoot tissue. The mean expression value over the three replicates is shown on a log10 transformation. D – differentially expressed gene ontologies. The exterior color of the bar splits root (blue) from the shoot (green), the fill color indicates the p-value level. The bars represent the average normalized expression value for the GO terms, based on all genes related to the GO term.

Figure 3. Gene ontology comparison between barley and tomato. A -Based on the expression values of genes annotated to a GO term, GO terms were merged between barley and tomato. A principal component analysis of all GO terms matched was performed, comparing all replicates of barley root, barley shoot, tomato root, and tomato shoot tissue to each other. B – the square rooted expression level of barley and tomato tissues for significantly different GO terms, indicated by the fill color of the bars.

663 **Figure 4.** Normalized expression (TMM) of photomorphogenesis controlling genes *Cry1* and *Cry2*. The
664 expression is compared between tissues (x-axis) and species (color).

665 **Figure 5.** Orthologous gene comparison between tomato and barley tissues. A – principal component
666 analysis of the orthologue genes, showing all three replicates for each tissue–species combination. B
667 – Classification of differentially expressed genes (DEG) and equally expressed genes (EEG) in the three
668 groups biological process, cellular component, and molecular function. The count of genes of each
669 group is illuminated. C – Circos plot of the normalized expression of shoot (green) and root, meristems
670 (brown) for tomato and barley, separated by chromosomes. Differentially expressed genes between
671 barley and tomato for the three groups photosynthesis (dark green), transport (gold), and translation
672 (dark red) are linked with lines in the center. D – similar to C, but showing the links between equally
673 expressed genes.

674

675 Supplementary information legends

676

677 **Suppl. Figure S1**. Workflow of the gene expression and functional analysis on three levels. Each level
678 is framed by a yellow, orange, or green square.

679 **Suppl. Figure S2**. The number of reads (in millions), mapped reads, and mapped in genes in Barley (A)
680 and tomato gene annotation (B).

681 **Suppl. Figure S3.** Correlations among three biological replicates of root apices (BRx / TRx) and shoot
682 apices (BSx/ TSx) in Barley (A) and tomato (B). Correlation is illustrated by color, shape, and additionally
683 as a numerical value.

684 **Suppl. Figure S4**. Gene ontology clustering results by applying AgriGo V2 - 51 significant GO terms have
685 been identified between the root and shoot meristem in barley. A – biological process; B – molecular
686 function; C - cellular component

687 **Suppl. Figure S5**. Gene ontology clustering results by applying AgriGo V2 - 63 significant GO terms have
688 been identified between the root and shoot meristem in tomato. A – biological process; B – molecular
689 function; C - cellular component

690 **Suppl. Figure S6.** Boxplot of the log10 transformed expression values for selected GO terms. Each dot
691 represents the expression level of a single gene, while the boxplot summarizes these single points.
692 Root and shoot are separated by color, while the species are spatially divided. Two statistical tests
693 were performed, between the tissues and between the species for each GO term individually. The
694 results of the tissue-wise comparison are printed below the GO term name between the green and
695 purple boxplots, while the species-related comparison is placed between the spatially separated
696 boxplots.

697 **Suppl. Figure S7**. Boxplot of the log10 transformed expression values for selected GO terms. Each dot
698 represents the expression level of a single gene, while the boxplot summarizes these single points.
699 Root and shoot are separated by color, while the species are spatially divided. Two statistical tests
700 were performed, between the tissues and between the species for each GO term individually. The
701 results of the tissue-wise comparison are printed below the GO term name between the green and
702 purple boxplots, while the species-related comparison is placed between the spatially separated
703 boxplots. The GO term and function are illustrated above each boxplot.

704 **Suppl. Figure S8.** Normalized expression (RPM) of photomorphogenesis controlling genes *Cry1* and
705 *Cry2*. The expression is compared between tissues (x-axis) and species (color). Expression data for
706 Morex, published by Liu et al. 2020 was added to compare barley expression patterns under short-day
707 (Scarlett – 8h) and long day (Morex – 16h) photoperiods.

708

709 **Suppl. Table 1.** Barley gene expression of normalized expression value. Basemean – mean expression
710 over all six replicates, BasemeanA – root mean value; BasemeanB – shoot mean value. PAdj –

711 Bonferroni adjusted p-value. BR_Rx – normalized expression values for each replicate separated BR =
712 barley root. BSM_Rx – normalized expression values for each replicate of the barley shoots separately.

713 **Suppl. Table 2.** Result of AgriGo V2 clustering of significantly expressed genes in barley root and shoot.

714 **Suppl. Table 3**. Barley gene ontology clustering based on expression values for each GO term.
715 Genecount – count of genes found for the GO term (identical between root and shoot); Avgr – Average
716 expression value root; SDr – standard deviation for root tissue; MINr / MAXr – minimum and maximum
717 expression values. Same presented for shoot tissue by Avgs, SDs, MINs and MAXs. Pval – probability
718 value calculated by a generalized linear model (binomial distribution). Logfc – Logfoldchange value.
719 FDR – adjusted p-value.

720 **Suppl. Table 4.** Tomato gene expression of normalized expression value. Basemean – mean expression
721 over all six replicates, BasemeanA – root mean value; BasemeanB – shoot mean value. PAdj –
722 Bonferroni adjusted p-value. TR_Rx – normalized expression values for each replicate separated TR =
723 tomato root. TSM_Rx – normalized expression values for each replicate of the tomato shoot
724 separately.

725 **Suppl. Table 5**. Result of AgriGo V2 clustering of significantly expressed genes in tomato root and
726 shoot.

727 **Suppl. Table 6**. Tomato gene ontology clustering based on expression values for each GO term.
728 Genecount – count of genes found for the GO term (identical between root and shoot); Avgr – Average
729 expression value root; SDr – standard deviation for root tissue; MINr / MAXr – minimum and maximum
730 expression values. Same presented for shoot tissue by Avgs, SDs, MINs and MAXs. Pval – probability
731 value calculated by a generalized linear model (binomial distribution). Logfc – Logfoldchange value.
732 FDR – adjusted p-value.

733 **Suppl. Table 7**. Orthologous genes (1 to1 relationship) identified by OrthoMCL analysis of protein
734 sequences between barley and tomato.

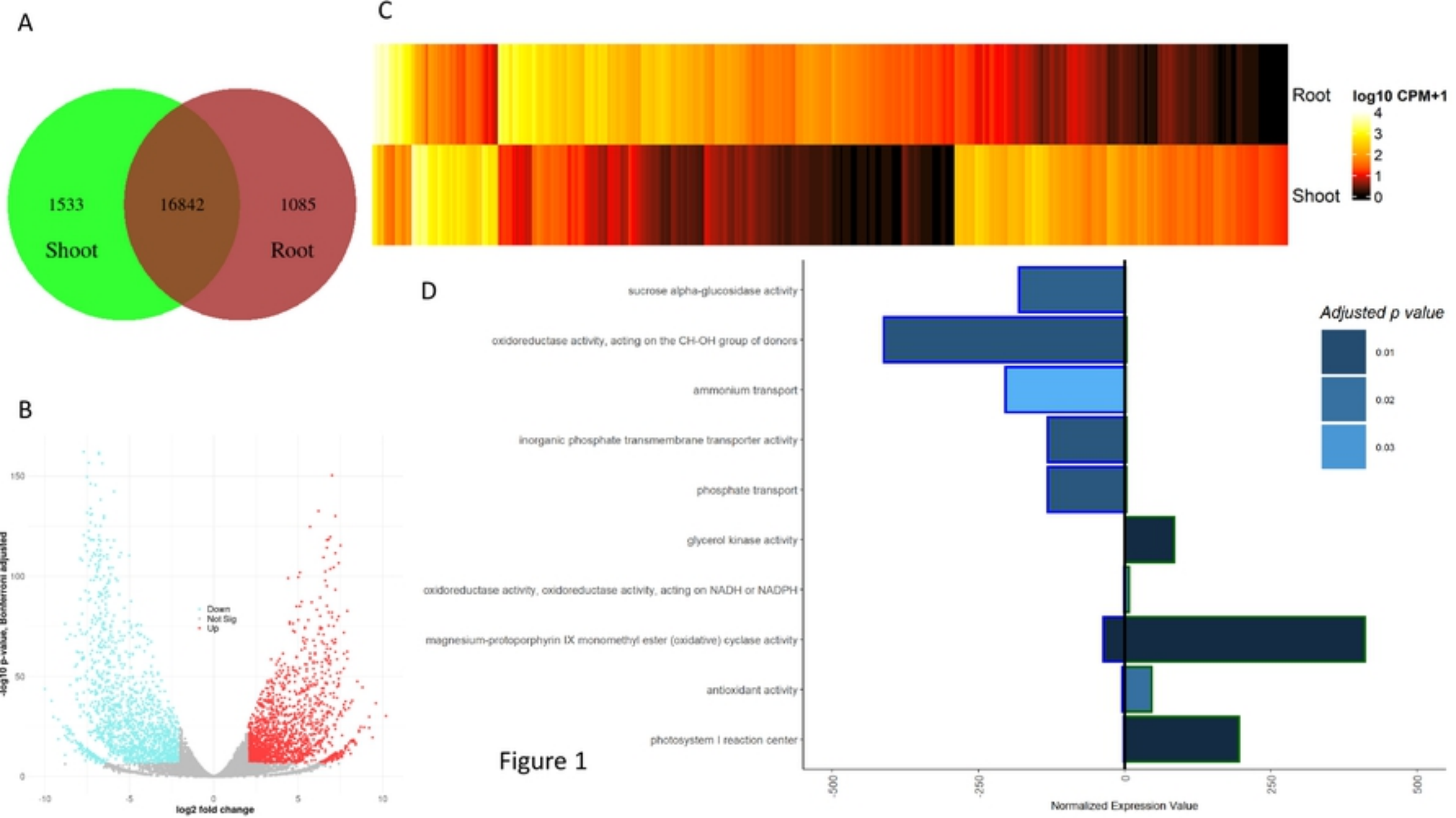
A
1533
16842
1085
Shoot
Root
B
Down
Not Sig
Up
-log10 p-value, Bonferroni adjusted
log2 fold change
C
Root
Shoot
log10 CPM+1
4
3
2
1
0
D
sucrose alpha-glucosidase activity
oxidoreductase activity, acting on the CH-OH group of donors
ammonium transport
inorganic phosphate transmembrane transporter activity
phosphate transport
glycerol kinase activity
oxidoreductase activity, oxidoreductase activity, acting on NADH or NADPH
magnesium-protoporphyrin IX monomethyl ester (oxidative) cyclase activity
antioxidant activity
photosystem I reaction center
Adjusted p value
0.01
0.02
0.03
Normalized Expression Value

Figure 1

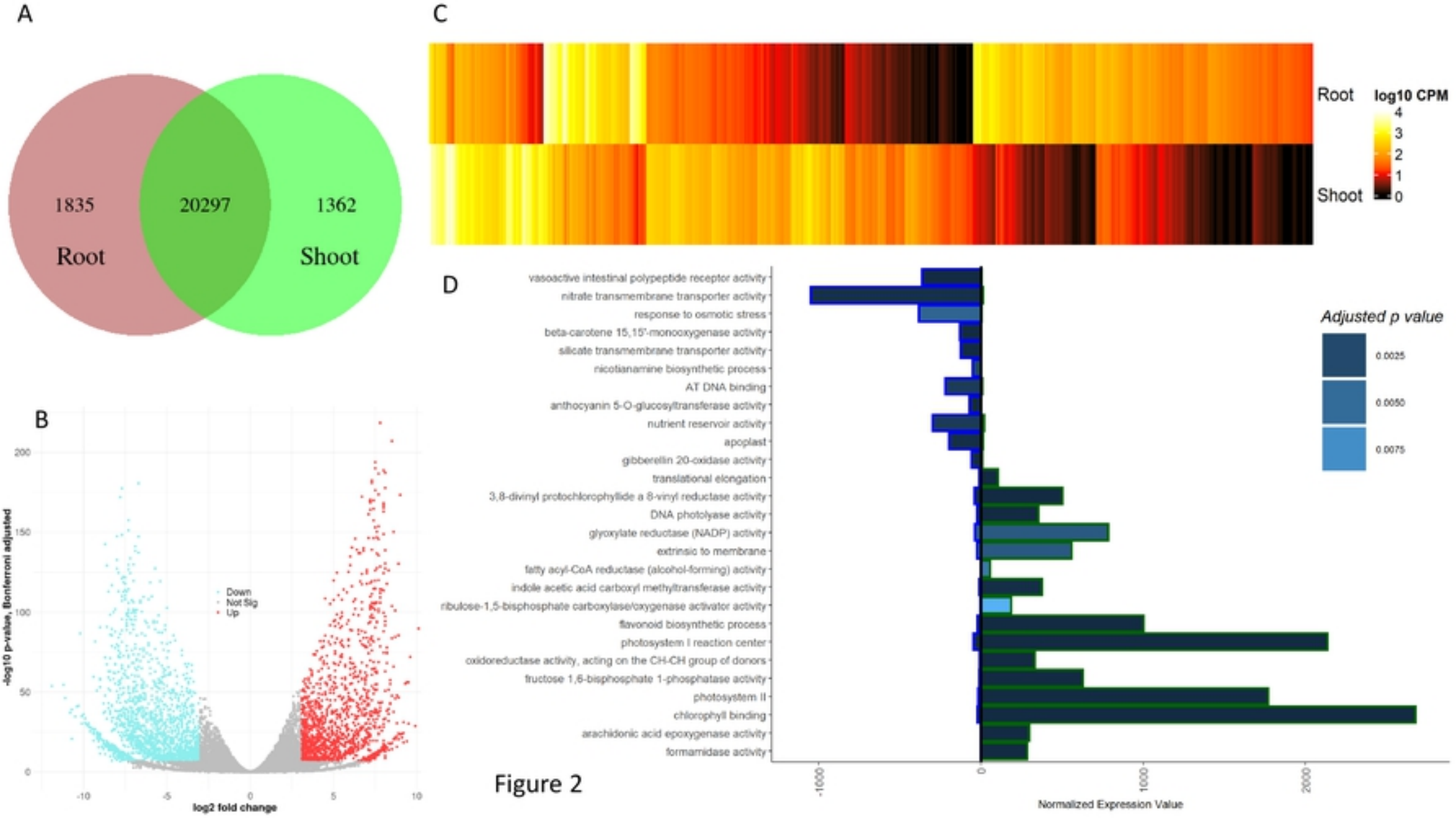
A
1835
20297
1362
Root
Shoot
B
Down
Not Sig
Up
-log10 p-value, Bonferroni adjusted
log2 fold change
C
Root
Shoot
log10 CPM
4
3
2
1
0
D
vasoactive intestinal polypeptide receptor activity
nitrate transmembrane transporter activity
response to osmotic stress
beta-carotene 15,15'-monooxygenase activity
silicate transmembrane transporter activity
nicotianamine biosynthetic process
AT DNA binding
anthocyanin 5-O-glucosyltransferase activity
nutrient reservoir activity
apoplast
gibberellin 20-oxidase activity
translational elongation
3,8-divinyl protochlorophyllide a 8-vinyl reductase activity
DNA photolyase activity
glyoxylate reductase (NADP) activity
extrinsic to membrane
fatty acyl-CoA reductase (alcohol-forming) activity
indole acetic acid carboxyl methyltransferase activity
ribulose-1,5-bisphosphate carboxylase/oxygenase activator activity
flavonoid biosynthetic process
photosystem I reaction center
oxidoreductase activity, acting on the CH-CH group of donors
fructose 1,6-bisphosphate 1-phosphatase activity
photosystem II
chlorophyll binding
arachidonic acid epoxygenase activity
formamidase activity
Adjusted p value
0.0025
0.0050
0.0075
Normalized Expression Value

Figure 2

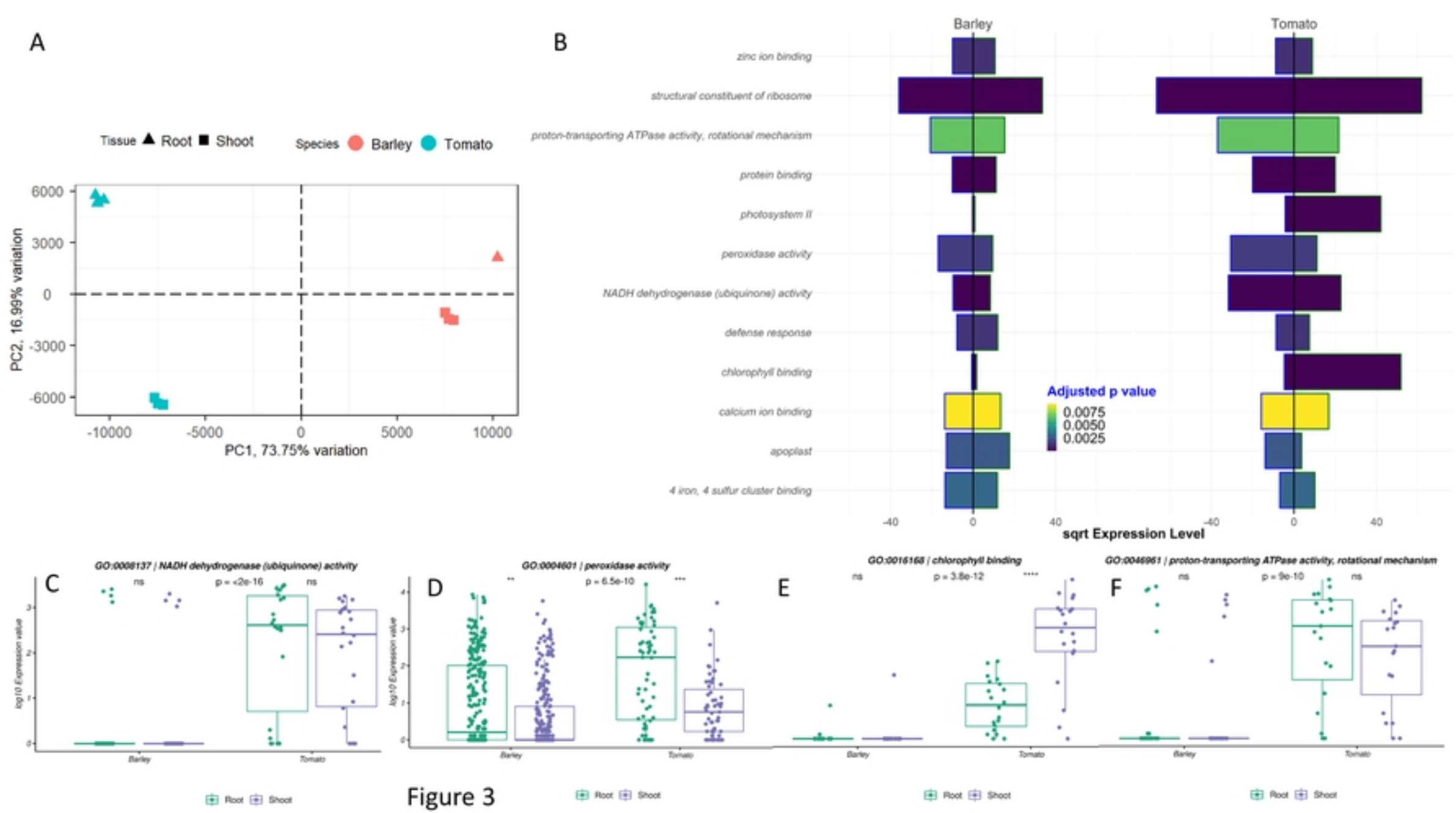
A
Tissue ▲ Root ■ Shoot
Species Barley Tomato
PC2, 16.99% variation
PC1, 73.75% variation
B
Barley
Tomato
zinc ion binding
structural constituent of ribosome
proton-transporting ATPase activity, rotational mechanism
protein binding
photosystem II
peroxidase activity
NADH dehydrogenase (ubiquinone) activity
defense response
chlorophyll binding
calcium ion binding
apoplast
4 iron, 4 sulfur cluster binding
Adjusted p value
0.0075
0.0050
0.0025
sqrt Expression Level
C
GO:0008137 | NADH dehydrogenase (ubiquinone) activity
D
GO:0004601 | peroxidase activity
E
GO:0016168 | chlorophyll binding
F
GO:0046961 | proton-transporting ATPase activity, rotational mechanism
log10 Expression value
Barley
Tomato
Root
Shoot

Figure 3

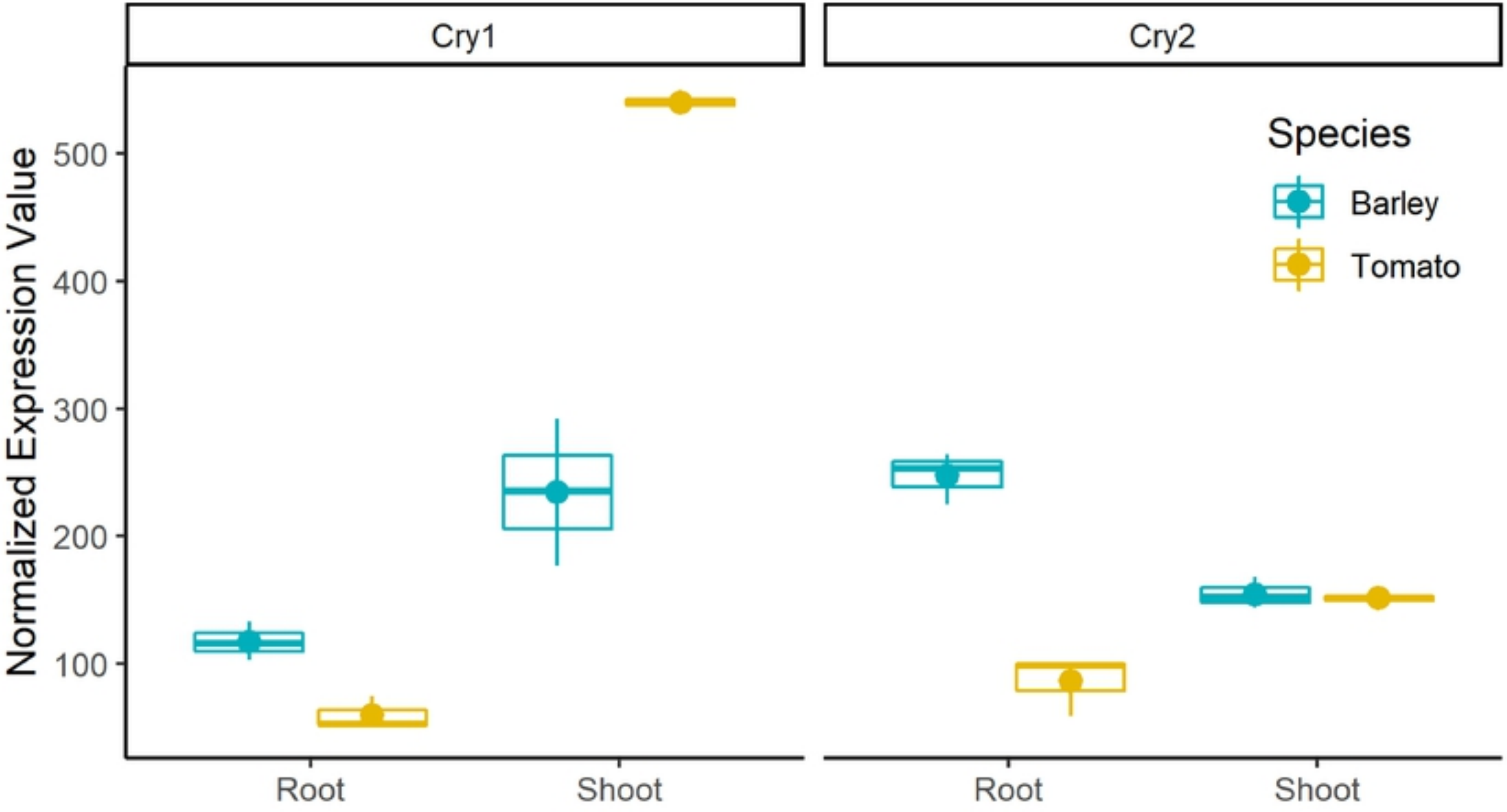
Cry1
Cry2
Species
Barley
Tomato
Normalized Expression Value
500
400
300
200
100
Root
Shoot
Root
Shoot

Figure 4

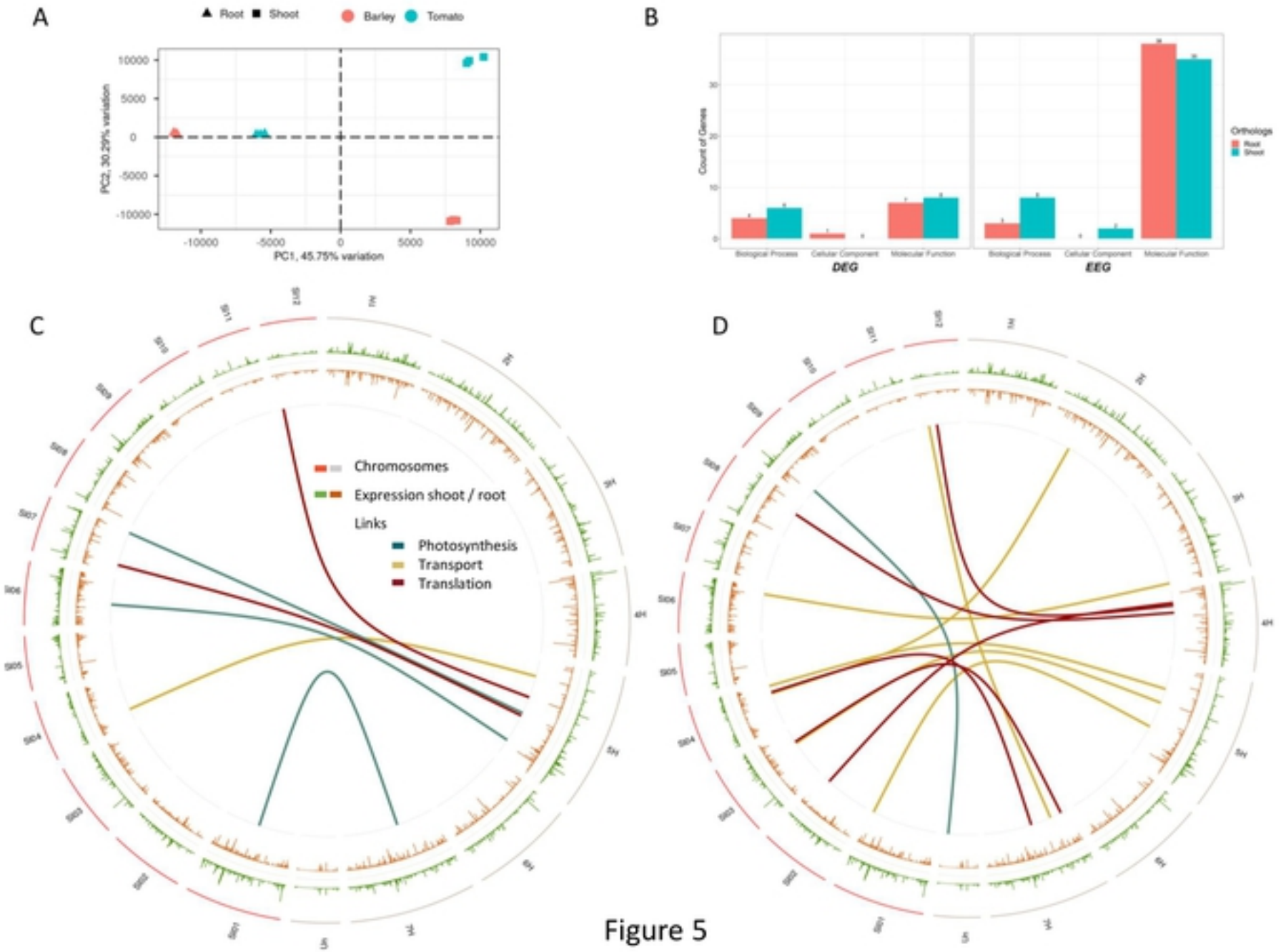
A
Root
Shoot
Barley
Tomato
PC2, 30.29% variation
PC1, 45.75% variation
B
Count of Genes
Orthologs
Root
Shoot
Biological Process
Cellular Component
Molecular Function
DEG
EEG
C
D
Chromosomes
Expression shoot / root
Links
Photosynthesis
Transport
Translation

Figure 5